ACS OMEGA

Article

Cite This: ACS Omega 2018, 3, 18466−18474

http://pubs.acs.org/journal/acsodf

Heterometallic Coordination Polymer Gels Supported by 2,4,6-Tris(pyrazol-1-yl)-1,3,5-triazine

Izar Capel Berdiell,* Alexander N. Kulak, Stuart L. Warriner, and Malcolm A. Halcrow*

School of Chemistry, University of Leeds, Woodhouse Lane, Leeds LS2 9JT, U.K.

Supporting Information

ABSTRACT: Complexes of type $[M(tpt)_2]X_2$ (M^{2+} = Fe^{2+}, Co^{2+}, Ni^{2+}; tpt = 2,4,6-tri{pyrazol-1-yl}-1,3,5-triazine; X^- = BF_4^- or ClO_4^-) crystallize in a cubic lattice, with the metal ion and ligand conformation showing unusual symmetry-imposed disorder. Addition of 1 equiv AgX to the corresponding preformed $[M(tpt)_2]X_2$ salt in concentrated $MeNO_2$ solution affords thixotropic gels. Gelation was not observed in analogous reactions using $[Mn(tpt)_2][ClO_4]_2$, or from reactions in other, more donating solvents. Scanning electron microscopy (SEM) images from dilute solutions of the reagents confirmed the fibrous microstructure of the gels and their homogeneous elemental composition. However, energy-dispersive X-ray data show a reduced Fe/Ag ratio compared to the Co/Ag and Ni/Ag gels, where a 1:1 ratio of metals is evident. More concentrated gels decomposed to silver nanoparticles during SEM sample preparation. Mass spectrometry and ^1H NMR indicate that silver induces partial ligand displacement reactions in $[Fe(tpt)_2]^{2+}$ and $[Co(tpt)_2]^{2+}$, but not in $[Ni(tpt)_2]^{2+}$. Hence, the strength of the gels, which follows the order M = Mn (no gel) < Fe < Co < Ni, correlates with the stability of octahedral $[M(tpt)_2]^{2+}$ under gelation conditions. Iron(II) complexes of the related ligands 2,4,6-tri{pyrazol-1-yl}pyridine (tpp) and 2,4,6-tri{pyrazol-1-yl}pyrimidine (tpym) did not undergo gelation with silver salts under the above conditions. The unique properties of tpt as a gelator in this work may reflect the crystallographically observed ability of metal-coordinated tpt to chelate to exogenous silver ions, through its pendant pyrazolyl group and triazinyl N donors. In contrast, the pendant azolyl substituents in silver complexes of the nongelators tpp and tpym only bind exogenous silver in monodentate fashion.

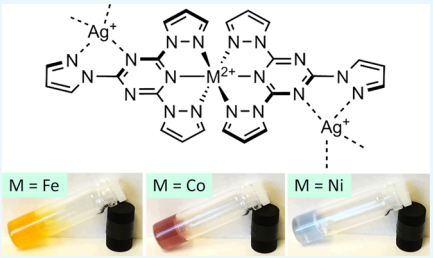

INTRODUCTION

Unravelling soft matter systems is a rich field of scientific investigation among chemists, physicists, and engineers. Over the last two decades, supramolecular gels have gained attention because of their potential applications in biomaterials, catalysis, displays, sensors, surface science, tissue engineering, and pollutant removal.[1−3] Supramolecular gels are usually formed by low-molecular-weight gelator molecules assembled in a 3D network, which traps a bulk amount of solvent via noncovalent interactions. The reversible and dynamic nature of the supramolecular interactions provides a mechanism for sensing or physical transformations in response to external stimuli.[2,3] More recently, coordination polymer gels (CPGs) or metallogels have also been widely reported, where metal ions play a crucial role in the assembly of the 3D network.[4−8] Inclusion of transition metals in the gel assembly brings tunability to the coordination strength, as well as new redox, optic, electronic, and magnetic properties which are intrinsic to the metal ion. These afford additional possibilities for applications in catalysis, luminescence, and adhesives as well as new types of sensing functionality.[7,8]

Silver(I)-containing metallogels of pyridyl-containing gelators are a particularly common class of CPG,[9−20] which can often template the formation of silver nanoparticles under mild heating or reduction.[13−20] CPGs of first-row transition ions are also often supported by pyridyl gelators,[9,11,21−33] but can also be prepared from more diverse organic scaffolds based on other heterocyclic N-donors, carboxylates, or other donor groups.[5−8,34−44] A handful of f-element CPGs have also been prepared, with emissive or self-healing properties.[45−47] In some cases, the organic components have been found to be selective gelators for particular metal ions or salts,[31,35] whereas rare examples of heterometallic CPGs have also been reported.[21,48]

2,4,6-Tri(pyrazolyl)-1,3,5-triazine (tpt, Chart 1) and its derivatives are well-known ligands for transition ions,[49−57] and we have recently investigated two aspects of the chemistry of tpt. The first is the spin state of $[Fe(tpt)_2]^{2+}$ (Chart 1, M = Fe), which is related to a well-known family of iron(II) spin-crossover (SCO) complexes.[56] The second are silver(I) complexes of tpt, which crystallize as 1D-coordination polymers of silver ions bridged by ditopic tpt ligands.[57] We therefore proposed $[Fe(tpt)_2]^{2+}$ centers might be linked into larger assemblies by coordination to exogenous silver ions. We now report a family of heterometallic CPGs derived by mixing preformed $[M(tpt)_2]X_2$ (M = Fe or another 3d metal ion; X^- = BF_4^- or ClO_4^-) with the corresponding silver(I) salt. To aid the interpretation of these results, complexes of two other, related ligands were also prepared and screened for silver-

Received: September 25, 2018
Accepted: December 13, 2018
Published: December 27, 2018

DOI: 10.1021/acsomega.8b02508
ACS Omega 2018, 3, 18466−18474

Chart 1. tpt Ligand, Its Hydrolysis Product bptOH, and the Geometry of the Precursor Complexes $[M(tpt)_2]^{2+}$ (M = Mn, Fe, Co, Ni, Cu)

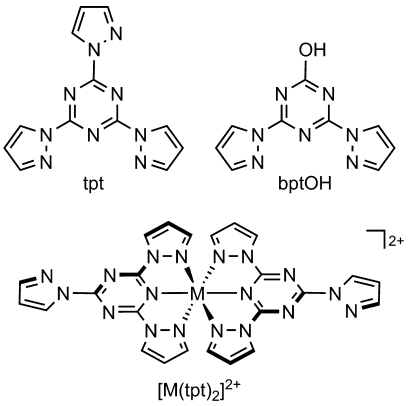

induced gelation behavior. Homometallic CPGs supported by a different trisubstituted 1,3,5-triazine scaffold have been described in a previous study.[58]

RESULTS AND DISCUSSION

The precursor complexes $[M(tpt)_2][BF_4]_2$ (M = Fe,[56] Co, Ni, Cu[55]) or $[M(tpt)_2][ClO_4]_2$ (M = Mn, Fe,[56] Ni) were prepared by reacting tpt with 0.5 equiv of the appropriate metal salt in nitromethane. The polycrystalline complexes were obtained after the usual work-up, and recrystallized from nitromethane using diethyl ether vapor as antisolvent. A full structure refinement of $[Ni(tpt)_2][BF_4]_2$ was achieved, which is isostructural with the major α-polymorph of $[Fe(tpt)_2][BF_4]_2$ (Figure 1 and Table S2).[56] The complex adopts the cubic space-group $Ia\bar{3}d$, with one-sixth of a six-coordinate complex molecule in its asymmetric unit and one unique C_3-symmetric ligand environment. The metal ion is distributed equally around the three N-donors of the unique triazinyl ring, with a concomitant twofold disorder of the coordinated pyrazolyl group. This symmetry-induced disorder yields a cubic lattice of tpt ligands, linked by a random array of nickel ions such that each tpt ligand coordinates only one metal atom (Figures S1 and S2). The triazinyl rings in the complex are sandwiched between two symmetry-equivalent BF_4^- ions, forming a typical anion···π interaction with a C···F distance of 2.756(8) Å (Figure S3).[55,59]

Crystals of the other Mn, Co, Ni, and Cu complex salts diffracted more weakly, but are isostructural with $[Ni(tpt)_2][BF_4]_2$ by X-ray powder diffraction (Figure 2 and Table S3). Samples of $[Cu(tpt)_2][BF_4]_2$ were often contaminated by other crystals, however, including $[Cu_2(tpt)_3(\mu\text{-bptO})(PzH)][BF_4]_3$, which was crystallographically characterized (Figure S4 and Table S4). The 2,4-dipyrazolyl-6-hydroxy-1,3,5-triazine (bptOH, Chart 1) and pyrazole (PzH) ligands in this complex are derived from hydrolysis of tpt during the crystallization process (Scheme S1), and their presence in the compound was confirmed by mass spectrometry (Figure S17). Although $[Cu(tpt)_2][BF_4]_2$ has previously been isolated in analytical purity,[55] copper(II) is known to promote hydrolysis of tpt under a variety of conditions owing to its high Lewis acidity.[53,54] Therefore, the following heterometallic gelation studies focus on the manganese, iron, cobalt, and nickel tpt complexes.

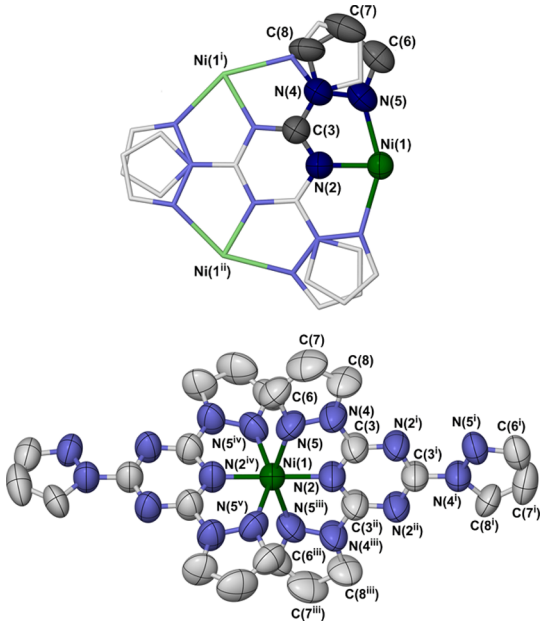

Figure 1. Top: ligand and metal-ion disorder in the structure of $[Ni(tpt)_2][BF_4]_2$. The atoms in the asymmetric unit are shown with 50% displacement ellipsoids, whereas their symmetry-equivalent atom sites are de-emphasized with paler coloration. Bottom: complete $[Ni(tpt)_2]^{2+}$ complex dication. Only one orientation of the disordered pendant pyrazolyl substituents is shown, and H atoms were omitted for clarity. Symmetry codes: (i) y, z, x; (ii) z, x, y; (iii) $1/4 - x, -1/4 + z, 1/4 - y$; (iv) $x, -y, 1/2 - z$; (v) $1/4 - x, -1/4 + z, 1/4 + y$. Color code: C, white or dark gray; Fe, pale or dark green; N, pale or dark blue.

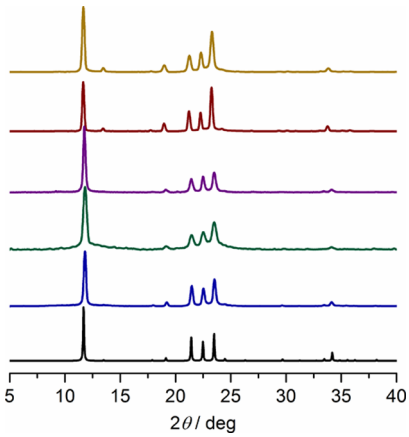

Figure 2. Experimental and simulated powder diffraction patterns of the compounds in this work: crystallographic simulation from α-$[Fe(tpt)_2][BF_4]_2$ (black); experimental data from $[Fe(tpt)_2][BF_4]_2$ (blue), $[Co(tpt)_2][BF_4]_2$ (cyan), $[Ni(tpt)_2][BF_4]_2$ (pink), $[Fe(tpt)_2][ClO_4]_2$ (red), and $[Ni(tpt)_2][ClO_4]_2$ (yellow). Unit cell parameters for these materials are given in Table S3.

Mononuclear $[M(tpt)_2]X_2$ was reacted with 1 equiv of the appropriate silver salt $AgBF_4$ or $AgClO_4$, in nitromethane. No reaction was observed when $[Mn(tpt)_2][ClO_4]_2$ was treated with $AgClO_4$. However, when M = Fe, Co, or Ni, thixotropic CPGs assembled within the time of mixing (Figure 3). Whereas the iron and cobalt gels show irreversible thixotropy, reverting to fluid solution upon mild shaking, the nickel-containing gels are more robust and remain viscous after shaking. The metal-dependence of gel stability qualitatively

DOI: 10.1021/acsomega.8b02508
ACS Omega 2018, 3, 18466−18474

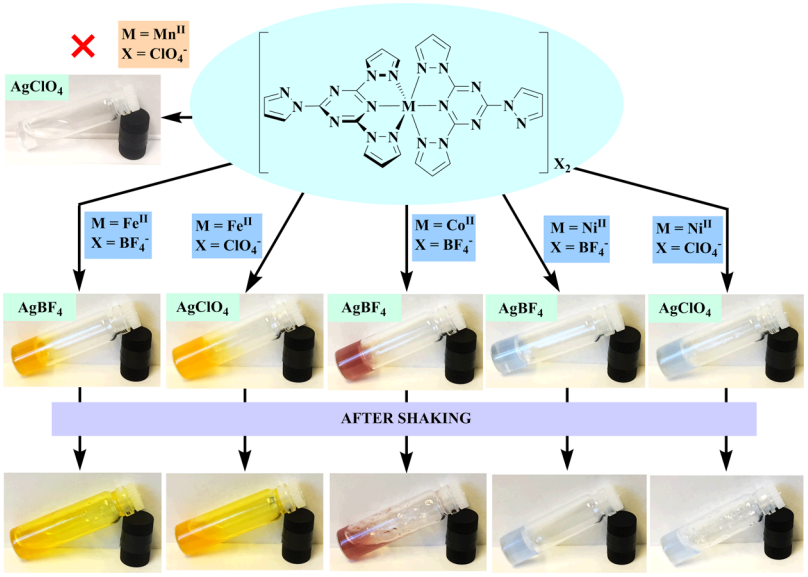

Figure 3. Heterometallic CPGs studied in this work.

follows the order M = Mn^{2+} < Fe^{2+} < Co^{2+} < Ni^{2+}, which corresponds to the Irving–Williams series for the strength of metal–ligand interactions.[60] The gels retain their viscosity when stored for a period of months at room temperature, in closed vials (Figure S5).

The gelation procedure was also attempted in the different solvents water, acetone, methanol, acetonitrile, and dimethylformamide. Although the mononuclear complexes are soluble in those solvents, the CPGs only assembled in nitromethane and at concentrations of at least 16 mg·cm^{-3} of $[M(tpt)_2]X_2$ and 12 mg·cm^{-3} AgX. The Ag/$[M(tpt)_2]^{2+}$ stoichiometry is also critical for gelation. When more than 1 equiv silver salt is used, the viscosity of the gel is reduced, and when 3 equiv silver(I) salt was added the gel did not assemble at all (Figure S6). Lastly, the gelation process is also affected by temperature, with gelation being enhanced if the components are mixed at 273 K and inhibited in reactions above 298 K. Once formed, however, the gels are thermostable up to ca. 330 K.

Scanning electron microscopy (SEM) images of the Fe/Ag, Co/Ag, and Ni/Ag CPGs were investigated. When dilute solutions of $[M(tpt)_2]X_2$ and AgX were evaporated to dryness under ambient conditions, networks of gel-like fibers of submicron thickness were observed (Figures 4 and S7). In contrast, if preassembled gel was evaporated to dryness, the SEM showed an amorphous material homogeneously distributed with silver nanoparticles (Figure S8). Hence, at higher concentrations the CPGs template the formation of silver nanoparticles when the solvent is removed. This is a common property of silver-containing CPGs.[13−20]

Energy-dispersive X-ray (EDX) mapping experiments proved the homogeneous distribution of the elements in the intact gels (Figures 5, S10, and S11). The Ag/M (M = Co or Ni) ratios in the $[Co(tpt)_2][BF_4]_2/AgBF_4$ and $[Ni(tpt)_2][BF_4]_2/AgBF_4$ gels were both quantified at 1:1.0 ± 0.1 from these data. The Ag/Fe ratio in $[Fe(tpt)_2][BF_4]_2/AgBF_4$ was lower however, at 1:4.1 ± 0.1, implying a reduced silver content in that CPG. That suggests the composition of the gels varies depending on the identity of the metal "M", despite their apparently similar microstructures.

Electrospray mass spectra of dilute $[Fe(tpt)_2]X_2/AgX$, $[Ni(tpt)_2]X_2/AgX$ (X^- = BF_4^- and ClO_4^-), and $[Co(tpt)_2][BF_4]_2/AgBF_4$ nitromethane solutions contain a mixture of M/tpt, Ag/tpt, and/or M/Ag/tpt-containing species (Figures S12–S16). The $[Fe(tpt)_2][BF_4]_2/AgBF_4$ and $[Ni(tpt)_2][ClO_4]_2/AgClO_4$ samples show particularly intense mixed-metal ions with general compositions $[MAg(tpt)_2Y_2]^+$, $[MAg_2(tpt)_mY_3]^+$, and $[M_2Ag(tpt)_mY_4]^+$ (m = 2 or 3; Y^- = anion), with an $[Fe_3Ag_3(tpt)_3Y_8]^+$ species also being observed in one case. This indicates association of the $[M(tpt)_2]^{2+}$ (M = Fe or Ni) and silver reagents into higher-order assemblies under these conditions, possibly with partial displacement of tpt from the iron or nickel centers. Spectra of BF_4^--containing

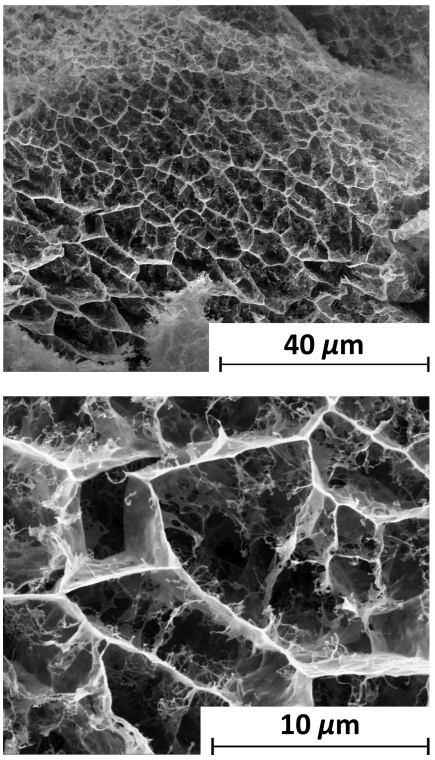

Figure 4. Two SEM images of the $[Ni(tpt)_2][BF_4]_2/AgBF_4$ CPG, showing the fibrous gel microstructure.

DOI: 10.1021/acsomega.8b02508
ACS Omega 2018, 3, 18466−18474

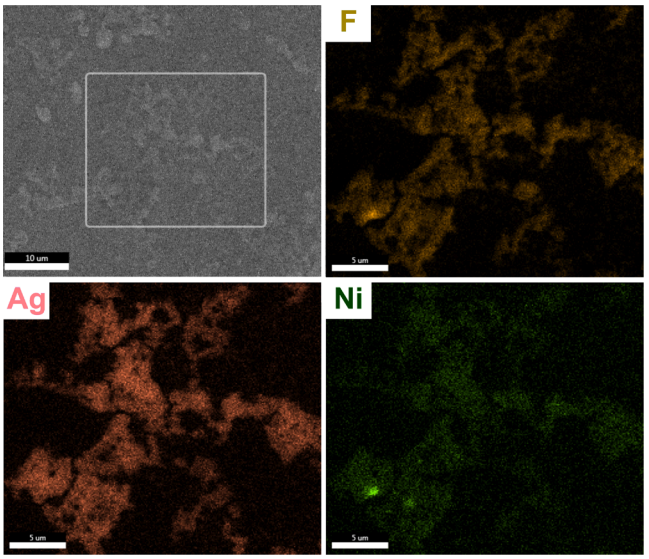

Figure 5. Fluorine, silver, and nickel EDX element maps for the $[Ni(tpt)_2][BF_4]_2/AgBF_4$ CPG.

gels also show ions containing the hydrolyzed tpt ligand fragment $[bptO]^-$ (Chart 1), which are not present in the ClO_4^--containing samples. That could reflect participation of F^-, produced by hydrolysis of BF_4^- inside the spectrometer, as a base or nucleophile in the hydrolysis reaction.[61]

^1H NMR data from similar mixtures in CD_3NO_2 contain one paramagnetic tpt ligand environment. For M = Fe and Co, addition of silver ions cleanly lowers the NMR symmetry of the tpt ligand from C_2 to C_1, which clearly indicates formation of a heterometallic M/Ag/tpt species. Additional peaks in the diamagnetic region also indicate the presence of metal-free tpt in these silver-containing solutions. Interestingly, for M = Ni (which forms the strongest gels) addition of silver has little effect on the paramagnetic or diamagnetic parts of the NMR spectrum (Figure 6). Hence, silver ions displace tpt ligands

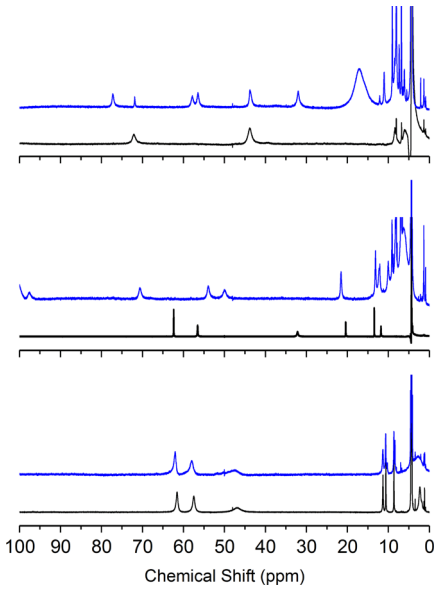

Figure 6. Comparison of the ^1H NMR spectra in CD_3NO_2 of pure $[M(tpt)_2][BF_4]_2$ (black) and a 1:1 mixture of $[M(tpt)_2][BF_4]_2$ and $AgBF_4$ (blue), for M = Fe (top), Co (center), and Ni (bottom).

from $[Fe(tpt)_2]^{2+}$ and $[Co(tpt)_2]^{2+}$ in CD_3NO_2 solution to form a new paramagnetic species, which is probably a heterometallic complex, but $[Ni(tpt)_2]^{2+}$ retains its integrity in the presence of silver ions under these conditions. That further supports the suggestion that the chemical structures of the $[M(tpt)_2]X_2/AgX$ CPGs depend on which "M" metal ion is present.

Our previous work demonstrated that $[Fe(tpt)_2]^{2+}$ is high-spin at room temperature, and remains so on cooling.[56] With the aim of producing a new form of gel with SCO switching properties,[62,63] iron complexes of tpt-analogue ligands based on di(pyrazol-1-yl)pyridine and di(pyrazol-1-yl)pyrimidine scaffolds were investigated (Chart 2). These ligand types are

Chart 2. Ligands tpp and tpym

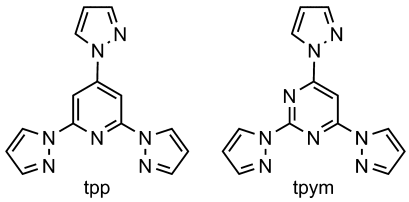

well-known to afford SCO iron(II) complexes.[64,65] Salts of $[Fe(tpp)_2]^{2+}$ (tpp = 2,4,6-tri{pyrazol-1-yl}pyridine) have been reported to exhibit SCO below room temperature in the solid state[64] and in solution,[66] but $[Fe(tpym)_2][BF_4]_2$ and $[Fe(tpym)_2][ClO_4]_2$ (tpym = 2,4,6-tri{pyrazol-1-yl}-pyrimidine)[67] were newly synthesized for this study. These salts of $[Fe(tpym)_2]^{2+}$ do not form isostructural crystals from nitromethane/diethyl ether, but both adopt the expected six-coordinate geometry with two pendant pyrazolyl groups per complex molecule (Figures S17, S18, and Table S4). The complexes were crystallographically high-spin at 120 K, which was confirmed by magnetic measurements showing them to be fully high-spin between 5 and 300 K (Figure S21). $[Fe(tpym)_2][BF_4]_2$ is also high-spin in CD_3CN solution, over the liquid range of that solvent (Figure S22). Hence, in contrast to a closely related compound,[65] tpym does not support SCO when bound to iron(II), which may reflect the inductive properties of its pendant pyrazolyl substituent on the tridentate ligand core.[66] Coordination of tpym to silver(I) yields dimeric or pentanuclear Ag/tpym molecular assemblies, containing $\mu,\kappa^1{:}\kappa^3$- or $\mu_3,\kappa^1{:}\kappa^2{:}\kappa^2$-tpym ligands.[57]

Neither $[Fe(tpp)_2]X_2$ nor $[Fe(tpym)_2]X_2$ (X^- = BF_4^- and ClO_4^-) formed gels when treated with 1 equiv AgX, under the conditions used to form the $[M(tpt)_2]^{2+}$-containing CPGs. Hence, silver-induced gelation appears to be a unique property of $[M(tpt)_2]^{2+}$ in this work.

DISCUSSION

Among the ligands in this work, only the $[M(tpt)_2]^{2+}$ scaffold supports gelation upon addition of silver. Moreover, the strength of the $[M(tpt)_2]X_2/AgX$ gels depends markedly on the metal "M", in the order Mn (no gel) < Fe < Co < Ni, and on the solvent present. The mass spectra imply ligand exchange reactions occur in the M/Ag/tpt mixtures, to form mixed-metal multinuclear species with a lower M/tpt stoichiometry. NMR data confirm that conclusion for M = Fe and Co, but not for M = Ni whose NMR spectrum is unchanged upon addition of silver. Hence, the robustness of the $[Ni(tpt)_2]X_2/AgX$ gels probably reflects the increased

DOI: 10.1021/acsomega.8b02508
ACS Omega 2018, 3, 18466−18474

stability of the $[Ni(tpt)_2]^{2+}$ center, which is consistent with the Irving–Williams series.[60] In that case, gelation of $[Ni(tpt)_2]X_2$/AgX occurs at concentrations high enough to promote weak coordination of silver ions to $[Ni(tpt)_2]^{2+}$, yielding $[Ag_n\{Ni(tpt)_2\}_n]^{3n+}$ oligomers with reasonably regular structures. Formation of the $[Fe(tpt)_2]X_2$/AgX and $[Co(tpt)_2]X_2$/AgX gels involves more complicated chemistry and, although these gels have similar morphologies and compositions to the Ni gels by SEM, their chemical structures may be more complex.

The reluctance of $[Fe(tpp)_2]X_2$ and $[Fe(tpym)_2]X_2$ to undergo silver-induced gelation might be understood from the structures of the homoleptic silver complexes of those ligands. Crystals of [Ag(tpt)]X (X^- = BF_4^- or ClO_4^-) have been obtained as 1D coordination polymers with helical or linear connectivities, with κ^2,κ^3:μ-tpt ligands (Figure S23).[57] That is, the tpt ligands in these structures chelate to both silver ions that are coordinated to them, through their pyrazolyl and triazinyl N donors. Several other 1,3,5-triazine derivatives can also bridge between silver ions in a similar fashion, at least in the solid state.[68−72] In contrast, [Ag(tpp)]X can only assemble into larger aggregates by monodentate binding through its pendant pyrazolyl substituent (Figure S24).[57] Moreover, although chelation of a second silver ion by tpym through the pyrimidinyl N1 atom and C6-pyrazolyl substituent is feasible in principle, this has not yet been observed in practice.[57] That may reflect a preferred transoid orientation of those N-donors, which avoids an intramolecular steric clash between the pyrimidinyl C4 and pyrazolyl C5 C−H groups (highlighted in red in Scheme 1). The transoid conformation is

Scheme 1. Cisoid and Transoid Conformations of the Pendant Pyrazolyl Substituent in Metal-Bound tpym. The Transoid Conformation is Present in Crystalline $[Fe(tpym)_2][ClO_4]_2{\cdot}n$MeNO$_2$

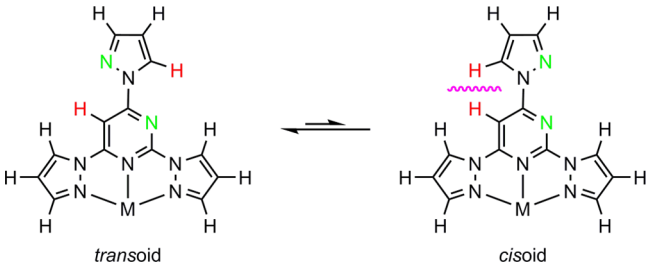

indeed observed crystallographically in $[Fe(tpym)_2][ClO_4]_2{\cdot}n$MeNO$_2$ (Figure S17; the pendant pyrazolyl conformation in the BF_4^- salt of this complex is uncertain because of symmetry-imposed crystallographic disorder).

Hence, of the ligands considered in this work, only tpt has a proven ability to chelate two silver ions simultaneously, which will afford more stable mixed-metal assemblies in solutions of $[M(tpt)_2]X_2$ and AgX. That might explain the unique gelation properties of the $[M(tpt)_2]X_2$/AgX system.

CONCLUSIONS

A new family of heterometallic, thixotropic CPGs is reported based on the potentially ditopic tpt gelator ligand, with the formula $\{[M(tpt)_2]X_2\}\{AgX\}_n$ (M^{2+} = Fe^{2+}, Co^{2+} or Ni^{2+}; X^- = BF_4^- or ClO_4^-; $n \leq 1$). The stability of the gels qualitatively correlates with the thermodynamic stability of the $[M(bpt)_2]^{2+}$ precursor complexes, according to the Irving–Williams series. Thus, the strongest and most thermally stable gels were obtained for M = Ni. SEM images showing the expected fibrous microstructures were obtained from dilute solutions of the gel components, with element mapping demonstrating their chemical homogeneity. However, EDX analyses imply that the M/Ag ratio in the gels, n, is smaller for M = Fe than for M = Co or Ni where approximately 1:1 ratios of these metals were observed. ^{1}H NMR also demonstrates that solutions of $[M(tpt)_2]X_2$ and AgX contain different species when M = Fe or Co, than for M = Ni (where the $[Ni(tpt)_2]^{2+}$ cation retains its integrity in the presence of silver ions). Hence, the chemical structure of the gels seems to vary depending on which "M" metal ion is present. The related complexes $[Fe(tpp)_2]^{2+}$ and $[Fe(tpym)_2]^{2+}$ do not form CPGs when combined with silver salts, which we attribute to their reduced ability to bind exogenous silver ions in a chelating (as opposed to monodentate) fashion. The current work aims to modify the gelator ligand structure further, to produce new thermochromic CPGs from SCO-active iron complex precursors.[73−76]

EXPERIMENTAL

Ligands tpt[77] and tpym,[67] and the complexes $[Cu(tpt)_2][BF_4]_2$,[55] $[Fe(tpt)_2]X_2$,[56] and $[Fe(tpp)_2]X_2$[64] (X^- = BF_4^- and ClO_4^-), were prepared following the literature procedures.

Synthesis of the Homoleptic Mononuclear Complexes. The following general procedure, as described for $[Co(tpt)_2][BF_4]_2$, was followed using appropriate amounts of the ligand and metal salt required for each product. Solutions of cobalt tetrafluoroborate hexahydrate (10 mg, 0.029 mmol) in nitromethane (20 cm^3), and of tpt (16 mg, 0.058 mmol) in nitromethane (15 cm^3), were mixed with stirring. The mixture was stirred for 5 min, then filtered. Addition of diethyl ether precipitated the product as a pale lilac powder, which was recrystallized from nitromethane/diethyl ether if required. Yields ranged from 50 to 85%. Characterization data for the complexes are as follows.

For $[Co(tpt)_2][BF_4]_2$. Elemental analysis for $C_{24}H_{18}B_2CoF_8N_{18}$ found (calcd) (%): C, 36.6 (36.4); H, 2.38 (2.29); N, 31.7 (31.9). ESMS m/z: 302.1 (10, $[Na(tpt)]^+$), 308.6 (100, $[Co(tpt)_2]^{2+}$). ^{1}H NMR (CD_3NO_2): δ 11.8, 13.4 (both 2H, pendant Pz H^3 and H^4), 20.4 (2H, pendant Pz H^5), 32.1 (4H, coordinated Pz H^5), 56.5 and 62.4 (both 4H, coordinated Pz H^3 and H^4).

For $[Ni(tpt)_2][BF_4]_2$. Elemental analysis for $C_{24}H_{18}B_2F_8N_{18}Ni$ found (calcd) (%): C, 36.4 (36.5); H, 2.12 (2.29); N, 31.7 (31.9). ^{1}H NMR (CD_3NO_2): δ 8.6, 10.6, 11.3 (all 2H, pendant Pz H^3–H^5), 46.9 (4H, coordinated Pz H^5), 55.5, 61.5 (both 4H, coordinated Pz H^3 and H^4).

For $[Ni(tpt)_2][ClO_4]_2$. Elemental analysis for $C_{24}H_{18}Cl_2N_{18}NiO_8$: found (calcd) (%): C, 35.2 (35.3); H, 2.15 (2.22); N, 30.8 (30.9). ESMS m/z: 280.1 (10, $[H(tpt)]^+$), 302.1 (25, $[Na(tpt)]^+$), 308.1 (100, $[Ni(tpt)_2]^{2+}$), 513.1 (12, [NiH(2,4-di(pyrazolyl)-6-hydroxo-1,3,5-triazine)(2,4-di-(pyrazolyl)-6-oxo-1,3,5-triazinate)]$^+$), 565.1 (15, [Ni(tpt)(2,4-di(pyrazolyl)-6-oxo-1,3,5-triazinate)]$^+$), 715.2 (9, $[Ni(tpt)_2(ClO_4)]^+$).

For $[Mn(tpt)_2][ClO_4]_2$. Elemental analysis for $C_{24}H_{18}Cl_2MnN_{18}O_8$: found (calcd) (%): C, 35.2 (35.5); H, 2.30 (2.23); N, 31.0 (31.0). ESMS m/z: 306.6 (100, $[Mn(tpt)_2]^{2+}$), 433.1 (65, $[Mn(tpt)(ClO_4)]^+$), 712.2 (19, $[Mn(tpt)_2(ClO_4)]^+$).

DOI: 10.1021/acsomega.8b02508
ACS Omega 2018, 3, 18466−18474

For $[Fe(tpym)_2][BF_4]_2$. Elemental analysis for $C_{26}H_{20}B_2F_8FeN_{16}$: found (calcd) (%): C, 39.5 (39.7); H, 2.61 (2.56); N, 28.3 (28.5). ESMS m/z: 306.1 (100, $[Fe(tpym)_2]^{2+}$), 369.1 (31, $[Fe(tpym)(H_2O)(OH)]^+$), 579.3 (8, $[Na(tpym)_2]^+$), 631.3 (5, $[Fe(tpym)_2F]^+$), 699.1 (6, $[Fe(tpym)_2(BF_4)]^+$). ^{1}H NMR (CD_3NO_2): δ 5.2, 6.4, 8.3 (all 2H, pendant Pz H^3–H^5), 42.2, 43.8, 44.4, 47.5 (all 2H, coordinated Pz H^4 and H^5), 60.8 (2H, Pym H^5), 73.7, 75.0 (both 2H, coordinated Pz H^3).

For $[Fe(tpym)_2][ClO_4]_2$. Elemental analysis for $C_{27}H_{23}Cl_2FeN_{17}O_{10}$ found (calcd) (%): C, 37.3 (37.2); H, 2.48 (2.66); N, 27.2 (27.3).

CAUTION! Although we have experienced no problems in handling the perchlorate salts in this study, metal–organic perchlorates are potentially explosive and should be handled with due care in small quantities.

Synthesis of the Gels. A silver tetrafluoroborate (3.1 mg, 0.016 mmol) solution in nitromethane (0.25 cm^3, corresponding to 12.4 mg·cm^{-3}) was added to a solution of $[Fe(tpt)_2][BF_4]_2$ in nitromethane (12.5 mg, 0.016 mmol in 0.7 cm^3; 17.9 mg·cm^{-3}). After brief stirring at room temperature, the CPG was formed. All the other CPG combinations were prepared in an analogous manner, using equimolar quantities of the appropriate complex and silver salt precursors.

Crystallography. All the crystals characterized in this study were obtained by slow diffusion of diethyl ether vapor into nitromethane solutions of the compounds. Crystallographic data were measured with an Agilent Supernova dual-source diffractometer, using monochromated Cu Kα (λ = 1.5418 Å) radiation. The diffractometer was fitted with an Oxford Cryostream low-temperature device. Experimental data (Table S1) and refinement procedures for the structure determinations are given in the Supporting Information. The structures were solved by direct methods (SHELXS97[78]) and developed by full least-squares refinement on F^2 (SHELXL97[78]). Crystallographic figures were prepared using XSEED,[79] and coordination volumes (V_{Oh}, Tables S2 and S4) were calculated using Olex2.[80]

Other Measurements. Electrospray mass spectra were obtained on a Bruker MicroTOF spectrometer, from nitromethane solution. Sodium cations and formate anions in the molecular ion assignments originate from calibrants in the spectrometer feed solutions. Elemental microanalyses were performed by the University of Leeds School of Chemistry microanalytical service or the London Metropolitan University microanalytical service. X-ray powder diffraction patterns were measured using a Bruker D2 Phaser diffractometer, with Cu Kα radiation (λ = 1.5418 Å). SEM images were obtained using an FEI Nova NanoSEM 450 environmental microscope, operating at 3 kV. A silicon wafer supporting the gel was mounted on an SEM stub using an adhesive copper film, then coated with iridium before imaging.

Magnetic susceptibility measurements were obtained using a Quantum Design SQUID magnetometer in an applied field of 5000 G. Diamagnetic corrections were estimated from Pascal's constants,[81] and a diamagnetic correction for the sample holder was also applied. Susceptibility measurements in solution were obtained by the Evans method using a Bruker DRX500 spectrometer operating at 500.13 MHz.[82,83] A diamagnetic correction for the sample[81] and a correction for the variation of the density of the CD_3CN solvent with temperature[84] were applied to these data.

■ ASSOCIATED CONTENT

Supporting Information

The Supporting Information is available free of charge on the ACS Publications website at DOI: 10.1021/acsomega.8b02508.

Experimental data, refinement procedures, additional figures and tabulated metric parameters for the crystal structure determinations; SEM images and EDX data from the gel samples; and X-ray powder diffraction, solid state and solution phase magnetic susceptibility measurements (PDF)

X-ray crystal structures: CCDC 1866452–1866455 (CIF)

■ AUTHOR INFORMATION

Corresponding Authors

*E-mail: cmic@leeds.ac.uk (I.C.B.).

*E-mail: m.a.halcrow@leeds.ac.uk (M.A.H.).

ORCID

Alexander N. Kulak: 0000-0002-2798-9301

Malcolm A. Halcrow: 0000-0001-7491-9034

Notes

The authors declare no competing financial interest.

Data associated with this study are available from the University of Leeds library at DOI: 10.5518/537.

■ ACKNOWLEDGMENTS

This work was funded by the Leverhulme Trust (RPG-2015-095) and by the EPSRC (EP/K00512X/1). The authors thank Drs. R. Kulmaczewski and O. Cespedes for help with the magnetic susceptibility measurements, and S. A. Barrett for the solution phase magnetic susceptibility data.

■ REFERENCES

(1) Dong, S.; Zheng, B.; Wang, F.; Huang, F. Supramolecular Polymers Constructed from Macrocycle-Based Host-Guest Molecular Recognition Motifs. *Acc. Chem. Res.* **2014**, *47*, 1982–1994.

(2) Babu, S. S.; Praveen, V. K.; Ajayaghosh, A. Functional π-Gelators and Their Applications. *Chem. Rev.* **2014**, *114*, 1973–2129.

(3) Jones, C. D.; Steed, J. W. Gels with Sense: Supramolecular Materials that Respond to Heat, Light and Sound. *Chem. Soc. Rev.* **2016**, *45*, 6546–6596.

(4) Piepenbrock, M.-O. M.; Lloyd, G. O.; Clarke, N.; Steed, J. W. Metal- and Anion-Binding Supramolecular Gels. *Chem. Rev.* **2010**, *110*, 1960–2004.

(5) Zhang, J.; Su, C.-Y. Metal-Organic Gels: from Discrete Metallogelators to Coordination Polymers. *Coord. Chem. Rev.* **2013**, *257*, 1373–1408.

(6) Tam, A. Y.-Y.; Yam, V. W.-W. Recent Advances in Metallogels. *Chem. Soc. Rev.* **2013**, *42*, 1540–1567.

(7) Jung, J. H.; Lee, J. H.; Silverman, J. R.; John, G. Coordination Polymer Gels with Important Environmental and Biological Applications. *Chem. Soc. Rev.* **2013**, *42*, 924–936.

(8) Sutar, P.; Maji, T. K. Coordination polymer gels: soft metal-organic supramolecular materials and versatile applications. *Chem. Commun.* **2016**, *52*, 8055–8074.

(9) Westcott, A.; Sumby, C. J.; Walshaw, R. D.; Hardie, M. J. Metallo-gels and organo-gels with tripodal cyclotriveratrylene-type and 1,3,5-substituted benzene-type ligands. *New J. Chem.* **2009**, *33*, 902–912.

(10) Xue, M.; Lü, Y.; Sun, Q.; Liu, K.; Liu, Z.; Sun, P. Ag(I)-Coordinated Supramolecular Metallogels Based on Schiff Base Ligands: Structural Characterization and Reversible Thixotropic Property. *Cryst. Growth Des.* **2015**, *15*, 5360–5367.

DOI: 10.1021/acsomega.8b02508
ACS Omega 2018, 3, 18466–18474

(11) Byrne, P.; Lloyd, G. O.; Applegarth, L.; Anderson, K. M.; Clarke, N.; Steed, J. W. Metal-induced gelation in dipyridyl ureas. *New J. Chem.* **2010**, *34*, 2261−2274.
(12) Wang, X.-Q.; Wang, W.; Yin, G.-Q.; Wang, Y.-X.; Zhang, C.-W.; Shi, J.-M.; Yu, Y.; Yang, H.-B. Cross-linked supramolecular polymer metallogels constructed via a self-sorting strategy and their multiple stimulus-response behaviors. *Chem. Commun.* **2015**, *51*, 16813−16816.
(13) Long, Q.; Peng, W.; Yuanwang, G.; Chunying, C.; Minghua, L. Self-Assembled Soft Nanomaterials via Silver(I)-Coordination: Nanotube, Nanofiber, and Remarkably Enhanced Antibacterial Effect. *Adv. Sci.* **2015**, *2*, 1500134.
(14) Piepenbrock, M.-O. M.; Clarke, N.; Steed, J. W. Rheology and Silver Nanoparticle Templating in a Bis(Urea) Silver Metallogel. *Soft Matter* **2011**, *7*, 2412−2418.
(15) Lee, J. H.; Kang, S.; Lee, J. Y.; Jung, J. H. A tetrazole-based metallogel induced with Ag^+ ion and its silver nanoparticle in catalysis. *Soft Matter* **2012**, *8*, 6557−6563.
(16) Rajamalli, P.; Malakar, P.; Atta, S.; Prasad, E. Metal induced gelation from pyridine cored poly(aryl ether) dendrons with in situ synthesis and stabilization of hybrid hydrogel composites. *Chem. Commun.* **2014**, *50*, 11023−11025.
(17) Liu, Z.-X.; Feng, Y.; Zhao, Z.-Y.; Yan, Z.-C.; He, Y.-M.; Luo, X.-J.; Liu, C.-Y.; Fan, Q.-H. A New Class of Dendritic Metallogels with Multiple Stimuli-Responsiveness and as Templates for the In Situ Synthesis of Silver Nanoparticles. *Chem.—Eur. J.* **2014**, *20*, 533−541.
(18) Paul, M.; Sarkar, K.; Dastidar, P. Metallogels Derived from Silver Coordination Polymers of C_3-Symmetric Tris(pyridylamide) Tripodal Ligands: Synthesis of Ag Nanoparticles and Catalysis. *Chem.—Eur. J.* **2015**, *21*, 255−268.
(19) Tatikonda, R.; Bertula, K.; Nonappa, N.; Hietala, S.; Rissanen, K.; Haukka, M. Bipyridine Based Metallogels: An Unprecedented Difference in Photochemical and Chemical Reduction in the In Situ Nanoparticle Formation. *Dalton Trans.* **2017**, *46*, 2793−2802.
(20) Sharma, M.; Sarma, P. J.; Goswami, M. J.; Bania, K. K. Metallogel Templated Synthesis and Stabilization of Silver-Particles and its Application in Catalytic Reduction of Nitro-arene. *J. Colloid Interface Sci.* **2017**, *490*, 529−541.
(21) Weng, W.; Beck, J. B.; Jamieson, A. M.; Rowan, S. J. Understanding the Mechanism of Gelation and Stimuli-Responsive Nature of a Class of Metallo-Supramolecular Gels. *J. Am. Chem. Soc.* **2006**, *128*, 11663−11672.
(22) Nath, K.; Husain, A.; Dastidar, P. Metallogels and Silver Nanoparticles Generated from a Series of Transition Metal-Based Coordination Polymers Derived from a New Bis-pyridyl-bis-amide Ligand and Various Carboxylates. *Cryst. Growth Des.* **2015**, *15*, 4635−4645.
(23) Piepenbrock, M.-O. M.; Clarke, N.; Steed, J. W. Metal Ion and Anion-Based "Tuning" of a Supramolecular Metallogel. *Langmuir* **2009**, *25*, 8451−8456.
(24) Adarsh, N. N.; Sahoo, P.; Dastidar, P. Is a Crystal Engineering Approach Useful in Designing Metallogels? A Case Study. *Cryst. Growth Des.* **2010**, *10*, 4976−4986.
(25) Dudek, M.; Clegg, J. K.; Glasson, C. R. K.; Kelly, N.; Gloe, K.; Gloe, K.; Kelling, A.; Buschmann, H.-J.; Jolliffe, K. A.; Lindoy, L. F.; Meehan, G. V. Interaction of Copper(II) with Ditopic Pyridyl-β-diketone Ligands: Dimeric, Framework, and Metallogel Structures. *Cryst. Growth Des.* **2011**, *11*, 1697−1704.
(26) Gee, W. J.; Batten, S. R. Instantaneous Gelation of a New Copper(II) Metallogel Amenable to Encapsulation of a Luminescent Lanthanide Cluster. *Chem. Commun.* **2012**, *48*, 4830−4832.
(27) Džolić, Z.; Cametti, M.; Milić, D.; Žinić, M. The Formation of $CuCl_2$-Specific Metallogels of Pyridyloxalamide Derivatives in Alcohols. *Chem.—Eur. J.* **2013**, *19*, 5411−5416.
(28) Sengupta, S.; Mondal, R. Elusive Nanoscale Metal-Organic-Particle-Supported Metallogel Formation Using a Nonconventional Chelating Pyridine-Pyrazole-Based Bis-Amide Ligand. *Chem.—Eur. J.* **2013**, *19*, 5537−5541.
(29) Fang, W.; Liu, C.; Chen, J.; Lu, Z.; Li, Z.-M.; Bao, X.; Tu, T. The Electronic Effects of Ligands on Metal-Coordination Geometry: a Key Role in the Visual Discrimination of Dimethylaminopyridine and its Application Towards Chemo-Switch. *Chem. Commun.* **2015**, *51*, 4267−4270.
(30) Kotova, O.; Daly, R.; dos Santos, C. M. G.; Kruger, P. E.; Boland, J. J.; Gunnlaugsson, T. Cross-Linking the Fibers of Supramolecular Gels Formed from a Tripodal Terpyridine Derived Ligand with d-Block Metal Ions. *Inorg. Chem.* **2015**, *54*, 7735−7741.
(31) Zhong, J.-L.; Jia, X.-J.; Liu, H.-J.; Luo, X.-Z.; Hong, S.-G.; Zhang, N.; Huang, J.-B. Self-assembled metallogels formed from N,N′,N″-tris(4-pyridyl)trimesic amide in aqueous solution induced by Fe(III)/Fe(II) ions. *Soft Matter* **2016**, *12*, 191−199.
(32) Arnedo-Sánchez, L.; Nonappa, N.; Bhowmik, S.; Hietala, S.; Puttreddy, R.; Lahtinen, M.; De Cola, L.; Rissanen, K. Rapid self-healing and anion selectivity in metallosupramolecular gels assisted by fluorine-fluorine interactions. *Dalton Trans.* **2017**, *46*, 7309−7316.
(33) Yu, X.; Wang, Z.; Li, Y.; Geng, L.; Ren, J.; Feng, G. Fluorescent and Electrochemical Supramolecular Coordination Polymer Hydrogels Formed from Ion-Tuned Self-Assembly of Small Bis-Terpyridine Monomer. *Inorg. Chem.* **2017**, *56*, 7512−7518.
(34) Wu, J.-J.; Cao, M.-L.; Zhang, J.-Y.; Ye, B.-H. A Nanocomposite Gel Based on 1D Coordination Polymers and Nanoclusters Reversibly Gelate Water Upon Heating. *RSC Adv.* **2012**, *2*, 12718−12723.
(35) Tanaka, K.; Yoshimura, T. A Novel Coordination Polymer Gel Based on Succinic Acid-Copper(II) Nitrate-DABCO: Metal Ion and Counterion Specific Organogelation. *New J. Chem.* **2012**, *36*, 1439−1441.
(36) Sarkar, S.; Dutta, S.; Chakrabarti, S.; Bairi, P.; Pal, T. Redox-Switchable Copper(I) Metallogel: A Metal-Organic Material for Selective and Naked-Eye Sensing of Picric Acid. *ACS Appl. Mater. Interfaces* **2014**, *6*, 6308−6316.
(37) Sarkar, S.; Dutta, S.; Bairi, P.; Pal, T. Redox-Responsive Copper(I) Metallogel: A Metal-Organic Hybrid Sorbent for Reductive Removal of Chromium(VI) from Aqueous Solution. *Langmuir* **2014**, *30*, 7833−7841.
(38) Qu, L.; Fan, J.; Ren, Y.; Xiong, K.; Yan, M.; Tuo, X.; Terech, P.; Royal, G. Homo- and Heterodinuclear Coordination Polymers Based on a Tritopic Cyclam Bis-Terpyridine Unit: Structure and Rheological Properties. *Mater. Chem. Phys.* **2015**, *153*, 54−62.
(39) Tang, S.; Olsen, B. D. Relaxation Processes in Supramolecular Metallogels Based on Histidine-Nickel Coordination Bonds. *Macromolecules* **2016**, *49*, 9163−9175.
(40) Sun, J.; Liu, Y.; Jin, L.; Chen, T.; Yin, B. Coordination-induced gelation of an l-glutamic acid Schiff base derivative: the anion effect and cyanide-specific selectivity. *Chem. Commun.* **2016**, *52*, 768−771.
(41) Feldner, T.; Häring, M.; Saha, S.; Esquena, J.; Banerjee, R.; Díaz, D. D. Supramolecular Metallogel That Imparts Self-Healing Properties to Other Gel Networks. *Chem. Mater.* **2016**, *28*, 3210−3217.
(42) Karan, C. K.; Bhattacharjee, M. Self-Healing and Moldable Metallogels as the Recyclable Materials for Selective Dye Adsorption and Separation. *ACS Appl. Mater. Interfaces* **2016**, *8*, 5526−5535.
(43) Ye, L.; Wan, L.; Huang, F. A Class of Polytriazole Metallogels via CuAAC Polymerization: Preparation and Properties. *New J. Chem.* **2017**, *41*, 4424−4430.
(44) Mitsumoto, K.; Cameron, J. M.; Wei, R.-J.; Nishikawa, H.; Shiga, T.; Nihei, M.; Newton, G. N.; Oshio, H. A Multi-Redox Responsive Cyanometalate-Based Metallogel. *Chem.—Eur. J.* **2017**, *23*, 1502−1506.
(45) Martínez-Calvo, M.; Kotova, O.; Möbius, M. E.; Bell, A. P.; McCabe, T.; Boland, J. J.; Gunnlaugsson, T. Healable Luminescent Self-Assembly Supramolecular Metallogels Possessing Lanthanide (Eu/Tb) Dependent Rheological and Morphological Properties. *J. Am. Chem. Soc.* **2015**, *137*, 1983−1992.
(46) McCarney, E. P.; Byrne, J. P.; Twamley, B.; Martínez-Calvo, M.; Ryan, G.; Möbius, M. E.; Gunnlaugsson, T. Self-Assembly Formation of a Healable Lanthanide Luminescent Supramolecular

DOI: 10.1021/acsomega.8b02508
ACS Omega 2018, 3, 18466−18474

Metallogel from 2,6-Bis(1,2,3-triazol-4-yl)pyridine (btp) ligands. *Chem. Commun.* **2015**, *51*, 14123−14126.
(47) Chen, P.; Li, Q.; Grindy, S.; Holten-Andersen, N. White-Light-Emitting Lanthanide Metallogels with Tunable Luminescence and Reversible Stimuli-Responsive Properties. *J. Am. Chem. Soc.* **2015**, *137*, 11590−11593.
(48) Zhang, J.; Chen, S.; Xiang, S.; Huang, J.; Chen, L.; Su, C.-Y. Heterometallic Coordination Polymer Gels Based on a Rigid, Bifunctional Ligand. *Chem.—Eur. J.* **2011**, *17*, 2369−2372.
(49) Guerrero, A.; Jalon, F. A.; Manzano, B. R.; Claramunt, R. M.; Cabildo, P.; Infantes, L.; Cano, F. H.; Elguero, J. The Structure of Tris(3′,5′-dimethylpyrazol-1-yl)-*s*-triazine and Its Use as a Ligand in Coordination Chemistry. *Chem. Heterocycl. Compd.* **2003**, *39*, 1396−1403.
(50) Zhou, H.-P.; Gan, X.-P.; Li, X.-L.; Liu, Z.-D.; Geng, W.-Q.; Zhou, F.-X.; Ke, W.-Z.; Wang, P.; Kong, L.; Hao, F.-Y.; Wu, J.-Y.; Tian, Y.-P. Anion-Induced Assembly of Five-Coordinated Mercury(II) Complexes and Density Functional Theory Calculations to Study Bond Dissociation Energies of Long Hg−N Bonds. *Cryst. Growth Des.* **2010**, *10*, 1767−1776.
(51) Gómez-de la Torre, F.; de la Hoz, A.; Jalón, F. A.; Manzano, B. R.; Otero, A.; Rodríguez, A. M.; Rodríguez-Pérez, M. C.; Echevarría, A.; Elguero, J. Synthesis and Characterization of Palladium(II) Complexes with New Polydentate Nitrogen Ligands. Dynamic Behavior Involving Pd−N Bond Rupture. X-ray Molecular Structure of $[\{Pd(\eta^3\text{-}C_4H_7)\}_2(\text{Me-BPzTO})](4\text{-}MeC_6H_4SO_3)$ [Me-BPzTO = 4,6-Bis(4-methylpyrazol-1-yl)-1,3,5-triazin-2-olate]. *Inorg. Chem.* **1998**, *37*, 6606−6614.
(52) Guerrero, A.; Jalón, F. A.; Manzano, B. R.; Rodríguez, A.; Claramunt, R. M.; Cornago, P.; Milata, V.; Elguero, J. Apparent Allyl Rotation in New Allylpalladium(II) Complexes with Pyrazolyl N-Donor Ligands. *Eur. J. Inorg. Chem.* **2004**, *2004*, 549−556.
(53) Manzur, J.; Acuña, C.; Vega, A.; García, A. M. Copper(II) assisted hydrolysis of 2,4,6-tris(pyrazol-1-yl)-1,3,5-triazine. Crystal and molecular structure of catena-$[CuL(H_2O)Cl]_n$ (L=2,4-dione-1,3,5-(1H)-triazin-1-amido). *Inorg. Chim. Acta* **2011**, *374*, 637−642.
(54) Wang, J.-X.; Wang, C.; Wang, X.; Wang, X.-Y.; Xing, Y.-H.; Sun, Q. Experimental and theoretical investigations of copper (I/II) complexes with triazine-pyrazole derivatives as ligands and their in situ C-N bond cleavage. *Spectrochim. Acta, Part A* **2015**, *142*, 55−61.
(55) Quiñonero, D.; Deyà, P. M.; Carranza, M. P.; Rodríguez, A. M.; Jalón, F. A.; Manzano, B. R. Experimental and computational study of the interplay between C-H/π and anion-π interactions. *Dalton Trans.* **2010**, *39*, 794−806.
(56) Capel Berdiell, I.; Kulmaczewski, R.; Halcrow, M. A. Iron(II) Complexes of 2,4-Dipyrazolyl-1,3,5-triazine Derivatives-The Influence of Ligand Geometry on Metal Ion Spin State. *Inorg. Chem.* **2017**, *56*, 8817−8828.
(57) Capel Berdiell, I.; Warriner, S. L.; Halcrow, M. A. Silver(i) complexes of bis- and tris-(pyrazolyl)azine derivatives—dimers, coordination polymers and a pentametallic assembly. *Dalton Trans.* **2018**, *47*, 5269−5278.
(58) Xing, B.; Choi, M.-F.; Xu, B. Design of Coordination Polymer Gels as Stable Catalytic Systems. *Chem.—Eur. J.* **2002**, *8*, 5028−5032.
(59) Gamez, P.; Reedijk, J. 1,3,5-Triazine-Based Synthons in Supramolecular Chemistry. *Eur. J. Inorg. Chem.* **2006**, *2006*, 29−42.
(60) Irving, H.; Williams, R. J. P. The stability of transition-metal complexes. *J. Chem. Soc.* **1953**, *1953*, 3192−3210.
(61) Esteban-Gómez, D.; Fabbrizzi, L.; Licchelli, M. Why, on Interaction of Urea-Based Receptors with Fluoride, Beautiful Colors Develop. *J. Org. Chem.* **2005**, *70*, 5717−5720.
(62) *Spin-Crossover Materials−Properties and Applications*; Halcrow, M. A., Ed.; John Wiley & Sons, Ltd.: New York, 2013; p 568.
(63) Gaspar, A. B.; Seredyuk, M. Spin Crossover in Soft Matter. *Coord. Chem. Rev.* **2014**, *268*, 41−58.
(64) Kershaw Cook, L. J.; Mohammed, R.; Sherborne, G.; Roberts, T. D.; Alvarez, S.; Halcrow, M. A. Spin State Behavior of Iron(II)/Dipyrazolylpyridine Complexes. New Insights From Crystallographic and Solution Measurements. *Coord. Chem. Rev.* **2015**, *289−290*, 2−12.
(65) Bushuev, M. B.; Krivopalov, V. P.; Nikolaenkova, E. B.; Daletsky, V. A.; Berezovskii, G. A.; Sheludyakova, L. A.; Varnek, V. A. Spin Crossover Complex $[FeL^1{}_2](ClO_4)_2{\cdot}H_2O$ (L^1 = 4-Methyl-2,6-bis(1*H*-pyrazol-1-yl)pyrimidine): Synthesis and Properties. *Polyhedron* **2012**, *43*, 81−88.
(66) Kershaw Cook, L. J.; Kulmaczewski, R.; Mohammed, R.; Dudley, S.; Barrett, S. A.; Little, M. A.; Deeth, R. J.; Halcrow, M. A. A Unified Treatment of the Relationship Between Ligand Substituents and Spin State in a Family of Iron(II) Complexes. *Angew. Chem., Int. Ed.* **2016**, *55*, 4327−4331.
(67) Gelling, A.; Noble, D. R.; Orrell, K. G.; Osborne, A. G.; Šik, V. Synthesis and Solution Fluxionality of Rhenium(I) Carbonyl Complexes of 2,4,6-Tris(pyrazolyl)pyrimidines (L), $[ReX(CO)_3L]$(X = Cl, Br or I). Isolation and Identification of the Dinuclear Complex $[\{ReBr(CO)_3\}_2L]$. *J. Chem. Soc., Dalton Trans.* **1996**, *1996*, 3065−3070.
(68) Bosch, E.; Barnes, C. L. One- and Two-Dimensional Silver-Coordination Networks Containing π-Sandwiched Silver−Silver Interactions. *Inorg. Chem.* **2002**, *41*, 2543−2547.
(69) Manzano, B. R.; Jalón, F. A.; Soriano, M. L.; Carrión, M. C.; Carranza, M. P.; Mereiter, K.; Rodríguez, A. M.; de la Hoz, A.; Sánchez-Migallón, A. Anion-Dependent Self-Assembly of Silver(I) and Diaminotriazines to Coordination Polymers: Non-Covalent Bonds and Role Interchange between Silver and Hydrogen Bonds. *Inorg. Chem.* **2008**, *47*, 8957−8971.
(70) Najafpour, M. M.; Hołyńska, M.; Amini, M.; Kazemi, S. H.; Lis, T.; Bagherzadeh, M. Two New Silver(I) Complexes With 2,4,6-Tris(2-pyridyl)-1,3,5-triazine (tptz): Preparation, Characterization, Crystal Structure and Alcohol Oxidation Activity in the Presence of Oxone. *Polyhedron* **2010**, *29*, 2837−2843.
(71) Hao, H.-J.; Sun, D.; Li, Y.-H.; Liu, F.-J.; Huang, R.-B.; Zheng, L.-S. Effect of Different Carboxylates on a Series of Ag(I) Coordination Compounds with Benzoguanamine Ligand. *Cryst. Growth Des.* **2011**, *11*, 3564−3578.
(72) Kelemu, S. W.; Steel, P. J. Highly Pyramidalised Hetero-aromatic Nitrogens in Discrete Multinuclear Silver(I) Complexes Assembled from Bis- And Tris-(diallylamino)azines. *CrystEngComm* **2013**, *15*, 9072−9079.
(73) Roubeau, O.; Colin, A.; Schmitt, V.; Clérac, R. Thermoreversible Gels as Magneto-Optical Switches. *Angew. Chem., Int. Ed.* **2004**, *43*, 3283−3286.
(74) Grondin, P.; Roubeau, O.; Castro, M.; Saadaoui, H.; Colin, A.; Clérac, R. Multifunctional Gels from Polymeric Spin-Crossover Metallo-Gelators. *Langmuir* **2010**, *26*, 5184−5195.
(75) Fujigaya, T.; Jiang, D.-L.; Aida, T. Spin-Crossover Physical Gels: A Quick Thermoreversible Response Assisted by Dynamic Self-Organization. *Chem.—Asian J.* **2007**, *2*, 106−113.
(76) Gural'skiy, I. A.; Reshetnikov, V. A.; Szebesczyk, A.; Gumienna-Kontecka, E.; Marynin, A. I.; Shylin, S. I.; V Ksenofontov, V.; Fritsky, I. O. Chiral Spin Crossover Nanoparticles and Gels with Switchable Circular Dichroism. *J. Mater. Chem. C* **2015**, *3*, 4737−4741.
(77) Claramunt, R.; Milata, V.; Cabildo, P.; Santa María, D.; Cornago, P.; Infantes, L.; Cano, F. H.; Elguero, J. 2,4,6-Tris(azol-1-yl)-1,3,5-triazines: A New Class of Multidentate Ligands. *Heterocycles* **2001**, *55*, 905−924.
(78) Sheldrick, G. M. Crystal structure refinement with SHELXL. *Acta Crystallogr., Sect. C: Struct. Chem.* **2015**, *71*, 3−8.
(79) Barbour, L. J. X-Seed—A Software Tool for Supramolecular Crystallography. *J. Supramol. Chem.* **2001**, *1*, 189−191.
(80) Dolomanov, O. V.; Bourhis, L. J.; Gildea, R. J.; Howard, J. A. K.; Puschmann, H. OLEX2: a Complete Structure Solution, Refinement and Analysis Program. *J. Appl. Crystallogr.* **2009**, *42*, 339−341.
(81) O'Connor, C. J. Magnetochemistry—Advances in Theory and Experimentation. *Prog. Inorg. Chem.* **1982**, *29*, 203−283.

DOI: 10.1021/acsomega.8b02508
ACS Omega 2018, 3, 18466−18474

(82) Evans, D. F. The determination of the paramagnetic susceptibility of substances in solution by nuclear magnetic resonance. *J. Chem. Soc.* **1959**, *1959*, 2003−2005.
(83) Schubert, E. M. Utilizing the Evans Method with a Superconducting NMR Spectrometer in the Undergraduate Laboratory. *J. Chem. Educ.* **1992**, *69*, 62.
(84) García, B.; Ortega, J. C. Excess viscosity .eta.E, excess volume VE, and excess free energy of activation .DELTA.G*E at 283, 293, 303, 313, and 323 K for mixtures acetonitrile and alkyl benzoates. *J. Chem. Eng. Data* **1988**, *33*, 200−204.

DOI: 10.1021/acsomega.8b02508
ACS Omega 2018, 3, 18466−18474